NEUROSCIENCE
RESEARCH ARTICLE
I. Puig-Parnau et al. / Neuroscience 512 (2023) 16–31

Intracranial Self-stimulation of the Medial Forebrain Bundle Ameliorates Memory Disturbances and Pathological Hallmarks in an Alzheimer's Disease Model by Intracerebral Administration of Amyloid-β in Rats

Irene Puig-Parnau,[a] Soleil Garcia-Brito,[b] Laia Vila-Soles,[b] Andrea Riberas,[a] Laura Aldavert-Vera,[b] Pilar Segura-Torres,[b]* Elisabet Kádár[a]* and Gemma Huguet[a]*

[a] *Universitat de Girona, Departament de Biologia, 17003 Girona, Spain*

[b] *Universitat Autònoma de Barcelona, Unitat Psicobiologia, Institut de Neurociències, 08193 Bellaterra, Barcelona, Spain*

Abstract—No curative or fully effective treatments are currently available for Alzheimer's disease (AD), the most common form of dementia. Electrical stimulation of deep brain areas has been proposed as a novel neuromodulatory therapeutic approach. Previous research from our lab demonstrates that intracranial self-stimulation (ICSS) targeting medial forebrain bundle (MFB) facilitates explicit and implicit learning and memory in rats with age or lesion-related memory impairment. At a molecular level, MFB-ICSS modulates the expression of plasticity and neuroprotection-related genes in memory-related brain areas. On this basis, we suggest that MFB could be a promising stimulation target for AD treatment. In this study, we aimed to assess the effects of MFB-ICSS on both explicit memory as well as the levels of neuropathological markers ptau and drebrin (DBN) in memory-related areas, in an AD rat model obtained by Aβ icv-injection. A total of 36 male rats were trained in the Morris water maze on days 26–30 after Aβ injection and tested on day 33. Results demonstrate that this Aβ model displayed spatial memory impairment in the retention test, accompanied by changes in the levels of DBN and ptau in lateral entorhinal cortex and hippocampus, resembling pathological alterations in early AD. Administration of MFB-ICSS treatment consisting of 5 post-training sessions to AD rats managed to reverse the memory deficits as well as the alteration in ptau and DBN levels. Thus, this paper reports both cognitive and molecular effects of a post-training reinforcing deep brain stimulation procedure in a sporadic AD model for the first time.

Key words: Alzheimer's disease, amyloid-β, deep brain stimulation, medial forebrain bundle, intracranial self-stimulation.

INTRODUCTION

Alzheimer's disease (AD) is the most common form of dementia. It is characterized by progressive wide-ranging cognitive and neuropsychiatric disturbances, among which episodic memory deficits are the earliest and most distinctive (Weintraub et al., 2012). At a molecular level, it is defined by the presence of amyloid-β (Aβ) plaques (Glenner and Wong, 1984) and tangles made of hyperphosphorylated tau (ptau) (Grundke-Iqbal et al., 1986a, 1986b). However, other neuropathological hallmarks, such as synaptic protein imbalance (e.g. reduced Debrin (DBN) levels), also appear early in the disease (Terry, 2000; Selkoe, 2002). The causative chain and hierarchy among them are still unknown.

No curative or fully effective treatments are currently available for AD (Alzheimer's Association, 2019). Electrical stimulation of deep brain areas (deep brain stimulation, DBS) has been suggested as a novel neuromodulatory approach to functionally restore memory circuits affected in AD (Lv et al., 2018). Results from initial clinical trials of DBS aimed at the nucleus basalis of Meynert or the fornix in AD patients, although promising, still pose some limitations regarding the extent and duration of its effects on cognitive aspects (Kuhn et al., 2015; Hardenacke et al., 2016; Lozano et al., 2016; Baldermann et al., 2018; Gratwicke et al., 2018). Yet, studies using experimental animals are exploring DBS effects on other brain regions in an attempt to further reveal potential targets of DBS for AD treatment (Aldehri et al., 2018; Yu et al., 2019).

Our group has consistently demonstrated that stimulation of the medial forebrain bundle (MFB), a part

*Corresponding authors.
E-mail addresses: pilar.segura@uab.es (P. Segura-Torres), elisabet.kadar@udg.edu, gemma.huguet@udg.edu (G. Huguet).
Abbreviations: AD, Alzheimer's disease; Aβ, Amyloid-β; DBS, Deep brain stimulation; MFB, Medial forebrain bundle; MWM, Morris water maze; Icv, Intracerebroventricular; ICSS, Intracranial self-stimulation.

https://doi.org/10.1016/j.neuroscience.2023.01.005
0306-4522/

of the neural substrate of reward, facilitates learning and memory in healthy and age or lesion-related memory impaired rats by means of intracranial self-stimulation (ICSS) (Aldavert-Vera et al., 1997; Segura-Torres et al., 1988, 2009; Redolar-Ripoll et al., 2002, 2003; Soriano-Mas et al., 2005 Ruiz-Medina et al., 2008a, 2008b; Kádár et al., 2014; García-Brito et al., 2017; Huguet et al., 2020). Furthermore, MFB-ICSS has been found to regulate the expression of synaptic plasticity proteins in the hippocampus and the retrosplenial cortex (Huguet et al., 2009, 2020; Kádár et al., 2011, 2013, 2016, 2018; Aldavert-Vera et al., 2013). Additionally, it has been shown to modulate the levels of hippocampal miRNAs described as key regulators of disturbed pathways in AD (Puig-Parnau et al., 2020). These results suggest that the MFB, which passes through the lateral hypothalamus, could be a promising stimulation target in AD treatment. Nevertheless, MFB-ICSS effects have never been evaluated in AD conditions.

An important handicap when testing treatments for AD is the lack of translationality of preclinical studies using experimental models (Cavanaugh et al., 2014; Zhang et al., 2019). In an attempt to overcome this limitation, the use of models mimicking sporadic onset AD (sAD), which accounts for about 95% of all AD cases (Zhang et al., 2019), is gaining popularity compared to more traditional transgenic models. In this regard, one of the most popular strategies used to mimic sAD relies on the delivery of amyloid-β (Aβ), the main constituent of the amyloid plaques, to the brain.

In this study, we aimed to assess whether the MFB-ICSS treatment in an AD rat model obtained by a single intracerebroventricular (icv) injection of Aβ aggregates, could alleviate both the spatial memory affectations and the alterations found in some molecular markers of early pathology. Specifically, we assess levels of ptau and DBN proteins in memory-related areas including the hippocampus and rhinal, retrosplenial and prelimbic cortices.

EXPERIMENTAL PROCEDURES

Animals and experimental design

A total of 36 adult male Wistar rats from our laboratory's breeding stock, with a mean age of 11.29 weeks (SD ± 0.68) and a mean weight of 368.63 g (SD ± 27.73) at the time of surgery, were used for this study. All procedures were approved by the University Animal Welfare Committee (CEEAH, protocol number 4848 P1), and were in compliance with the European Community Council Directive (86/609/CEE, 92/65/CEE, 2010/63/UE), Royal Decree 53/201.

Rats were individually housed in a controlled environment (20–24 °C temperature, 40–70% humidity, 12-h light/dark cycle) and were allowed free access to water and rodent chow.

As further described in the following sections, rats were intracerebroventricularly (icv)-infused with oligomerized Aβ or vehicle and implanted with a monopolar electrode aimed at the MFB on day 0. The animals were then trained on the Morris water maze (MWM) task between day 26 and 30 and tested for spatial memory 72 h after the training phase, on day 33. After the probe test, the rats were euthanized for molecular characterization. The ICSS treatment was administered immediately after each MWM acquisition session (experimental timeline shown in Fig. 1).

Thus, a total of four groups were considered (Aβ: Aβ-injected rats that receive sham treatment; Aβ + ICSS: Aβ-injected rats that receive ICSS treatment; VEH: vehicle-injected rats that receive sham treatment, and ICSS: vehicle-injected rats that receive ICSS treatment). One subject was eliminated from the Aβ + ICSS group due to an unrelated illness and one subject was eliminated from the ICSS group due to technical issues during the stimulation treatment. The final sample sizes were as follows: Aβ: $n = 10$; Aβ + ICSS: $n = 9$; VEH: $n = 8$, and ICSS: $n = 7$.

Preparation and assessment of Aβ oligomeric aggregates

To prepare amyloid-β toxic oligomers for icv injection, amyloid-β protein fragment 1–42 (Sigma A9810) was pre-treated with HFIP (Sigma 105228-5G) in order to obtain a pre-aggregate free solution, by overnight incubation at 0.2 mM. After that, aliquots containing 3.75 nmol of amyloid-β were divided into Eppendorf tubes and HFIP was then removed by overnight evaporation followed by 1.5 h in an exsiccator attached to a vacuum inlet. Aliquots of dried peptide film were stored at −80 °C until use. On day −7, dried peptide was dissolved in PBS pH 7.4 (DPBS Lonza Biowhitaker) and the solution (25 μM) was then sonicated in a standard bath sonicator for 5 min and incubated at 37 °C for 168 h in order to obtain oligomeric aggregates. Before use on day 0, each aliquot was subsequently diluted with PBS to the final injection concentration of 15 μM.

The presence of oligomeric aggregates in the injected sample was assessed via Western blot. Twenty-eight μL of amyloid-β peptide prepared identically to the ones to be injected (15 μM) were loaded onto a Criterion TGX Stain-Free PreCast Gels 4–15% polyacrylamide (Bio-Rad) lane and electrotransferred to PVDF membrane. After 1 h of blocking with 5% Bovine Serum Albumin (Sigma) in TBS-T (tris-buffered saline [100 mM NaCl, 10 mM Tris-HCl, pH 7.5] containing 0.1% Tween-20), membrane was incubated with rabbit anti-amyloid-β H31L21 primary antibody (1: 1,000, # 700,254 Thermofisher) at 4 °C, overnight. Goat anti-rabbit peroxidase-conjugated secondary antibody was used for 1 h at room temperature (1:20,000, no. 31460, ThermoScientific). Antibody reactive bands were detected using Immobilon Western Chemiluminescent HRP Substrate (EMD Millipore) in a FluorChem luminometer.

Intracerebroventricular injection of amyloid-β

Rats were anesthetized using an intraperitoneal injection of ketamine and xylazine (110 mg/kg Ketolar® ketamine chlorhydrate (Parke-Davis S.L. Pfizer, Madrid, Spain)

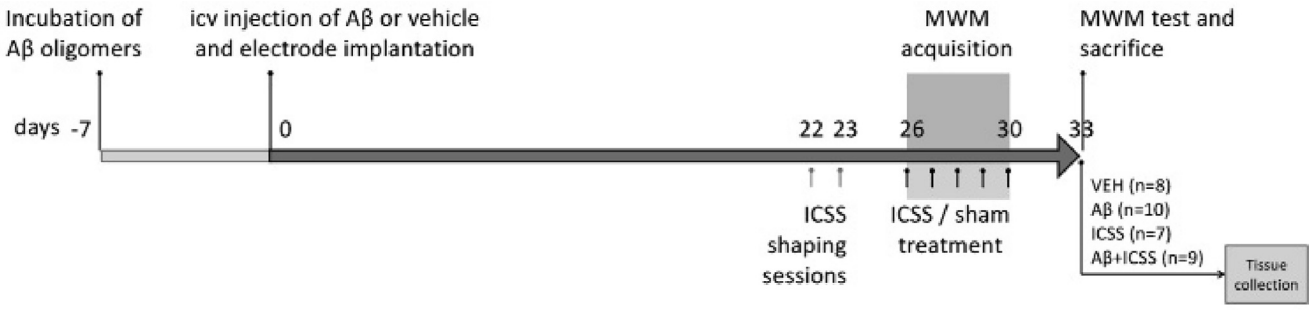

Fig. 1. Timeline of the experimental design. On day 0, rats were icv infused with oligomerized Aβ or vehicle and implanted with a monopolar electrode aimed at the MFB. Animals were trained on the MWM task between day 26 and 30 and sacrificed on day 33 post-injection. Animals in Aβ + ICSS and ICSS groups receive ICSS treatment after each MWM acquisition session, while Aβ and VEH groups receive sham treatment instead.

and 0.08 ml/100 g Rompun® xylazine 23 mg/ml; i.p. (Bayer, Barcelona, Spain). With the animal set on a stereotactic apparatus, a midline incision was made using a scalpel, from the frontal cranial bones to the back of the parietal cranial bones, to expose the dorsal surface of the skull. Two small perforations were drilled in the skull, at AP = -0.7 mm and L = −1.6/+1.6 mm from Bregma, according to stereotaxic atlas (Paxinos and Watson, 2006). For rats in Aβ and Aβ + ICSS groups, 10 μL of Aβ1-42 oligomeric preparation at 15 μM was bilaterally injected icv (2x5 μL) with a 10 μL Hamilton syringe penetrating at DV = -4.00 mm. The infusion was made over about 7 minutes (rate of 0.7 μL/minute) and retained 3 minutes to allow for complete diffusion of drug (total of 10 minutes per hemisphere). The amount of Aβ1-42 injected at the concentration of 15 μM in each case equaled 0.677 μg of Aβ peptide per rat. Rats in vehicle groups (VEH and ICSS groups) underwent the same procedures except that only PBS was injected.

Electrode implantation

Right after icv injection and still set in the stereotactic apparatus, rats were chronically implanted with an ICSS electrode aimed at the MFB in the lateral hypothalamus at coordinates from Bregma: AP = -2.3 mm; ML = 2.0 mm, in the right hemisphere (ipsi hemisphere); and DV = -8.8 mm (Paxinos and Watson, 2006). The electrode device consisted of a single-channel system with ground, manufactured in our laboratory, with two electrodes connected and welded on the two terminals of a female micro connector (acquired in microelectronics stores, 34 mm × 80 mm). The electrode to be implanted at the MFB, was a 200 μm diameter insulated stainless steel strain wire (008-SW PlasticsOne). The ground electrode was a copper wire that was welded to one of the screws anchored in the skull during the stereotaxic intervention. The electrode device was anchored to the skull with 4 jeweler's screws and dental cement, and the incision site was stitched up, allowing easy access to the protruding connector.

During the post-surgery recovery period (7 days), the animals were weighed and handled daily and a protocol for animal welfare supervision was applied during the whole procedure.

Intracranial self-stimulation treatment

ICSS shaping session took place on days 22 and 23 after Aβ injection, when animals randomly assigned to the ICSS experimental condition were taught to self-stimulate by pressing a lever in a conventional Skinner box (25 × 20 × 20 cm^3). Electrical brain stimulation consisted of 0.3 sec trains of 50 Hz sinusoidal waves at intensities ranging from 40 to 170 μA. The optimum current intensity (OI) was established for each rat as the mean of the two current intensities producing the highest response rate in the two shaping sessions (responses/min).

ICSS treatment consisted of 5 sessions (1 session/day for 5 consecutive days), administered immediately after each MWM acquisition session. During each session, rats in Aβ + ICSS and ICSS groups were placed in a self-stimulation box and were free to press the lever to self-administer 2500 trains of electrical stimulation at the established OI for each subject. Sham rats (Aβ and VEH groups) were handled and allowed to explore the ICSS box for 30 minutes but did not receive any electrical stimulation.

Morris water maze

Spatial learning and memory were assessed using the MWM task, in a 2 m diameter pool. A configuration of distinctive objects (lights, boxes, toys, balls, etc.) was used to provide distal visual cues for the animals to locate themselves within the tank and in reference to the escape platform (escape target), regardless of the entry point. All animals were given one habituation session and one 4-trial cued session 72 h prior to the first acquisition session in order to reduce emotional reactivity and test the animals' ability to swim to the cued goal (Vorhees and Williams, 2010).

Rats were given 5 MWM acquisition sessions, one per day on days 26–30, each of which consisted of 4 trials, with a mean intertrial interval of 120 sec. Each trial consisted of one swim from the edge of the pool to the platform set in the middle of the target quadrant, starting from one of the four different cardinal points in a semi-

random schedule. If a rat failed to find the platform within 90 sec, it was kindly guided to it, left there for 15 sec and removed from the pool. Otherwise, when animals found the platform before the completion of the trial, they were left on it for 15–30 sec and then were removed by the experimenter. The probe test, during which the platform was removed, was performed 72 h after the last acquisition session. The animal was introduced to the pool from the starting position and allowed to swim for 60 sec. All swim paths were recorded using a closed-circuit video camera (Smart Video Tracking System, Version 2.5, Panlab).

Tissue collection

Immediately after the probe test, animals were euthanized by decapitation. Ipsilateral (right) brain hemispheres were collected and fixed in 4% formaldehyde in 0.01 M PBS for 24 hours. Post-fixed entire hemispheres were cryopreserved in sucrose 15% 0.01 M PBS at 4 °C for 48 h, followed by another 48 h in sucrose 30% 0.01 M PBS at 4 °C, and finally frozen using freeze aerosol and stored at −80 °C until cryotomy. Serial coronal sections of 35 μm in thickness were obtained in a cryostat (Reichert-Jung Cryocut 1800, with 2020 microtome) at −25 °C from the coordinates between Bregma −2.50 and −3.80 (for parietal-temporal lobe sections) and between Bregma 2.00 and 3.50 (for frontal lobe sections). Sections were collected into Eppendorf tubes and stored at −80 °C until their use for free-floating immunohistochemistry.

Ptau and DBN immunostaining

Free-floating sections were set in 24-well plates in TBS [50 mM Tris; 150 mM NaCl; pH 7,6]. Sections for both DBN (post-fixed in 2% formaldehyde in TBS for 20 min) and ptau immunostaining were incubated in 0.3% H_2O_2 in 0.5% triton TBS (TBS-T) for 40 min to block endogenous peroxidase and then in 7% normal goat serum (Vector S-1000, in TBS-T) for 1 h at room temperature. After that, sections were incubated in primary antibody (Rabbit anti-DBN1, ABN207, EMD Millipore, 1: 3,000 for 4 h at room temperature followed by 1 overnight at 4 °C or Mouse anti-ptau AT8, MN1020, ThermoScientific, 1:200 for 4 h at room temperature followed by overnight at 4 °C, 1 h at room temperature and another overnight at 4 °C), washed in TBS-T and incubated with biotinylated secondary antibody (Goat anti-rabbit IgG Biotin, 111-066-144, Jackson Immunoresearch. 1:600 or Goat anti-mouse IgG Biotin, 115-065-166, Jackson Immunoresearch. 1:600) for 1.5 h at room temperature. After washing, sections were incubated in ABC (diluted 1/3 in TBS-T, Vectastain Elite ABC-Peroxidase kit, PK-6100, Vector) for 35 min. They were then incubated in DAB (SK-4100, Vector Labs) prepared according to the manufacturer's instructions, without nickel. Sections were mounted onto gelatinized slides and left to dry overnight. Finally, sections were subsequently dehydrated in ethanol 50% (2 × 3 min), 70% (2 × 3 min), 96% (3 × 3 min) and 100% (2 × 5 min), placed in HistoClear (2 × 5 min) and cover-slipped in Pertex medium (Sigma, Alddrich).

Photomicrographs of hippocampal region, rhinal cortices and retrosplenial cortex, as well as for prelimbic cortex were obtained from parietal-temporal sections (Bregma −2.50 to −3.80) and frontal sections (Bregma 2.00–3.50), respectively (Figs. 2A and 3A), using an Olympus Vanox-T AH-2 microscope attached to an Olympus DP73 digital camera, using a 2× objective.

ImageJ was used to quantify immunolabelling intensity. Mean intensity values were measured in regions of interest (ROIs) set at the different layers and subregions for each specific region (Figs. 2B and 3B).

Statistical analyses

All statistical analyses were performed using IBM SPSS Statistics 25. Normality analyses were performed for data of each group using the Shapiro-Wilk normality test. The Student's t-test was used to assess the effect of icv infusion of Aβ oligomers and ANOVA analyses were applied to assess the ICSS effect in rats with or without icv Aβ infusion. Additionally, a 2 × 5 mixed GLM was conducted to study the mean latency in the MWM acquisition phase using GROUP, SESSION and GROUP × SESSION as main factors. Correlations between variables were estimated using the Spearman's correlation test. The Hedge's g or Spearman's correlation coefficient (ρ) were used to measure the effect size. Statistically significant results were considered when $p < 0.05$ using 95% confidence interval.

RESULTS

Aggregation of Aβ1-42 peptide

Different bands, corresponding to different oligomeric species of Aβ (dimers, trimers and tetramers), were revealed between 8 and 20 kDa, indicating the presence of soluble toxic Aβ1–42 species in the injected solution (Fig. 4).

Fig. 2. Photomicrograph analysis for DBN and ptau immunostaining in parietal-temporal sections. (A) Location of photomicrographs for analysed regions in a parietal-temporal section (-3.60 mm from Bregma). Areas covered by photomicrographs are shown with rectangular frames, which are indistinctly drawn in the different hemispheres only for clarification. **(B)** Location of regions of interest (ROIs) employed to quantify labelling intensity levels in each of the analysed regions, shown superimposed in blue in a DBN (left) and ptau (right) stained parietal-temporal section. Area selected for the threshold measure, imposed for ptau analysis, is shown in red. In black, the different regionalization of each area is shown, according to Paxinos and Watson's atlas (Paxinos and Watson, 2006). Scale bar = 500 μm. Abbreviations: cc: corpus callosum; cg: cingulum; DG: dentate gyrus; Ect: ectorhinal cortex; hil: hilus; HP: hippocampus; IP: infrapyramidale; Lent: lateral entorhinal cortex; Pir; piriform cortex; PRh: perirhinal cortex; RhC: rhinal cortices; RSA: retrosplenial agranular cortex; RSC: retrosplenial cortex; RSG: retrosplenial granular cortex; SLM: stratum lacunosum moleculare; SO: stratum oriens; SP: suprapyramidale; SR: stratum radiatum.

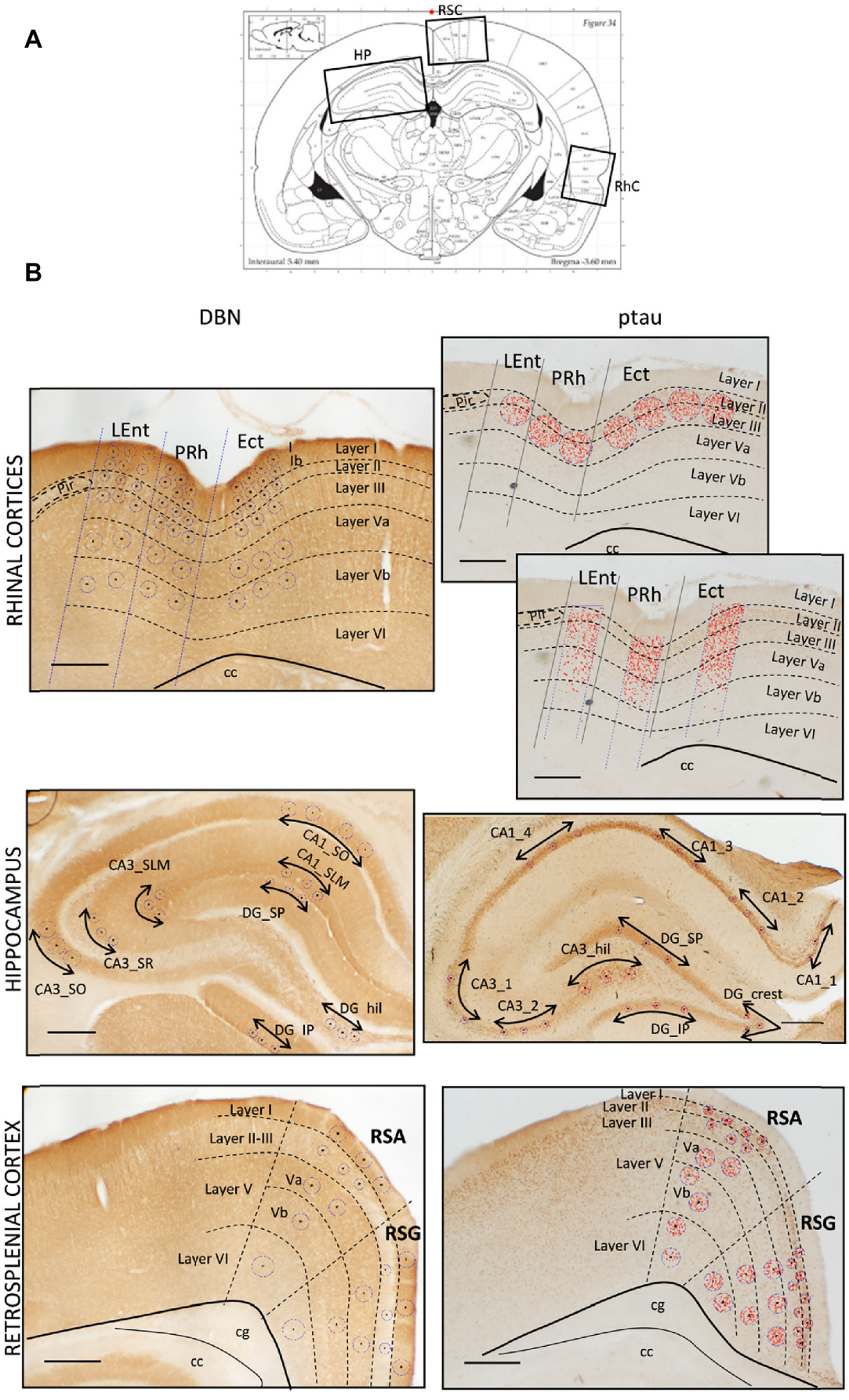
A
RSC
HP
RhC
Figure 34
Interaural 5.40 mm
Bregma -3.60 mm
B
DBN
ptau
RHINAL CORTICES
LEnt
PRh
Ect
Pir
I
Ib
Layer I
Layer II
Layer III
Layer Va
Layer Vb
Layer VI
cc
HIPPOCAMPUS
CA3_SLM
CA1_SO
CA1_SLM
DG_SP
CA3_SR
CA3_SO
DG_hil
DG_IP
CA1_4
CA1_3
CA1_2
CA3_hil
CA3_1
CA3_2
CA1_1
DG_crest
RETROSPLENIAL CORTEX
Layer I
Layer II-III
Layer V
Va
Vb
Layer VI
RSA
RSG
cg
cc

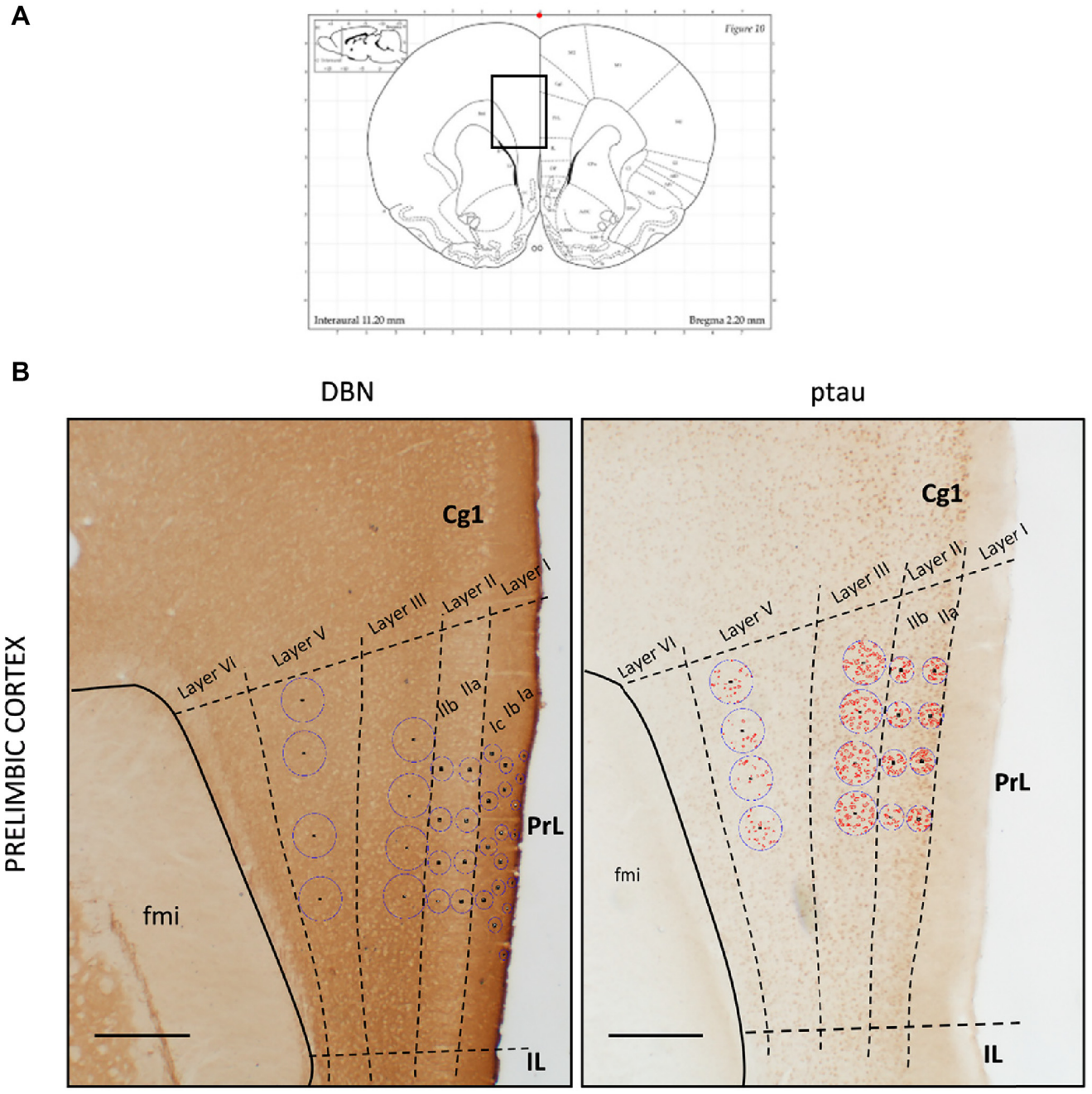

Fig. 3. Photomicrograph analysis for DBN and ptau immunostaining in frontal sections. (A) Location of photomicrographs for prelimbic cortex analysis in a frontal section (+2.20 mm from Bregma). **(B)** Location of regions of interest (ROIs) employed to quantify labelling intensity levels in each of the analysed layers, shown superimposed in blue, in a DBN (left) and ptau (right) stained frontal section. Area selected for the thresholded measure, imposed for ptau analysis, is shown in red. In black, the different regionalization of medial prefrontal cortex is shown, according to Paxinos and Watson's atlas (Paxinos and Watson, 2006). Scale bar = 500 μm. Abbreviations: Cg1: cingulate cortex area1; fmi: forceps minor of the corpus callosum; IL: infralimbic cortex; PrL: prelimbic cortex. Different bands, corresponding to different oligomeric species of Aβ (dimers, trimers and tetramers), were revealed between 8 and 20 kDa, indicating the presence of soluble toxic Aβ1–42 species in the injected solution (Fig. 4).

Electrode location and ICSS behaviour

Fig. 5 shows the location of the tip of the electrodes of the subjects who received ICSS (ICSS and Aβ + ICSS groups). In all animals, the tip of the electrode was located in the MFB, anywhere between anteroposterior coordinates −1.8 mm and −2.56 mm in reference to Bregma.

No significant differences were observed between the ICSS and Aβ + ICSS groups in terms of ICSS behaviour. Specifically, the administration of Aβ did not affect any of the following parameters: the optimal intensity of stimulation (ICSS: 130.71 μA; Aβ + ICSS: 121.11 μA), the maximum response rate (ICSS: 60.14 responses/min; Aβ + ICSS: 72.55 responses/min), the average

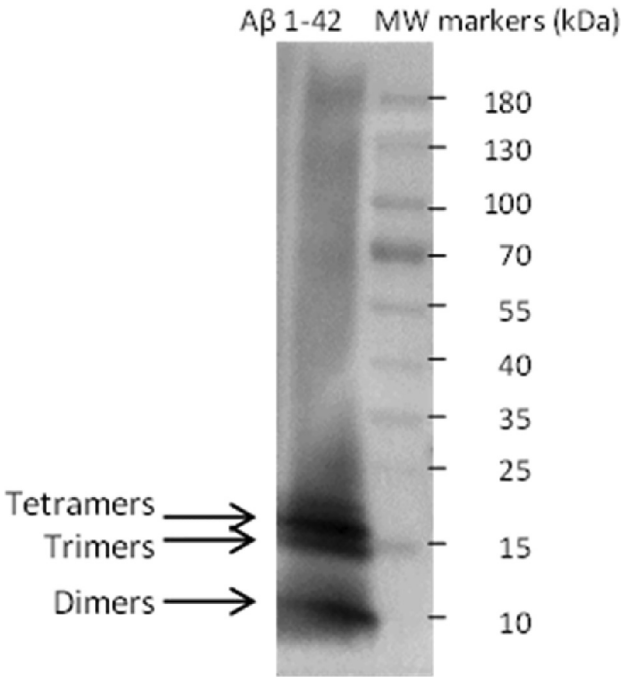

Fig. 4. Aggregation state of injected amyloid-β peptide. Western blot of Aβ solution to be injected: sonicated Aβ 1–42 peptide dilution (25 μM in PBS) was incubated for 168 h at 37 °C and diluted to 15 μM before loading the sample on PAGE and transfering it onto a PVDF membrane, probed with amyloid-β monoclonal antibody H31L21, revealing the presence of Aβ aggregates of 8–20 kDa (dimers, trimers and tetramers). Molecular weight standards are indicated on the right.

time that it took the subjects to administer the 2500 stimulation trains of the post-training treatment (ICSS: 38.85 min; Aβ + ICSS: 37.35 min).

Spatial learning and memory

Spatial learning curves according to escape latencies across the different acquisition sessions in the MWM for the four experimental groups, are depicted in Fig. 6. Statistical analysis showed an interaction GROUP × SESSION [$F_{12,120}$ = 1.876, p < 0.05)], indicating that the profile was not the same for all groups. The ICSS group differs the most from the rest, presenting a descending linear evolution of greater slope than that of the Aβ + ICSS (p = 0.027) and VEH (p = 0.050) groups. This facilitative effect of ICSS treatment on the acquisition in rats without Aβ became evident in session 3, where the ICSS group presented lower latencies than those of the VEH group (p = 0.032; g = 1.085). Differences between groups diminished in the last two sessions.

Conversely, no differences were observed in the evolution of learning between the Aβ group and the Aβ + ICSS and vehicle groups. Furthermore, group Aβ also showed a significant decrease in performance between the first and the last training session, indicating that all groups learned the task (p < 0.001 for all groups). In fact, there were no significant effects of Aβ on the acquisition and short-term memory of the task.

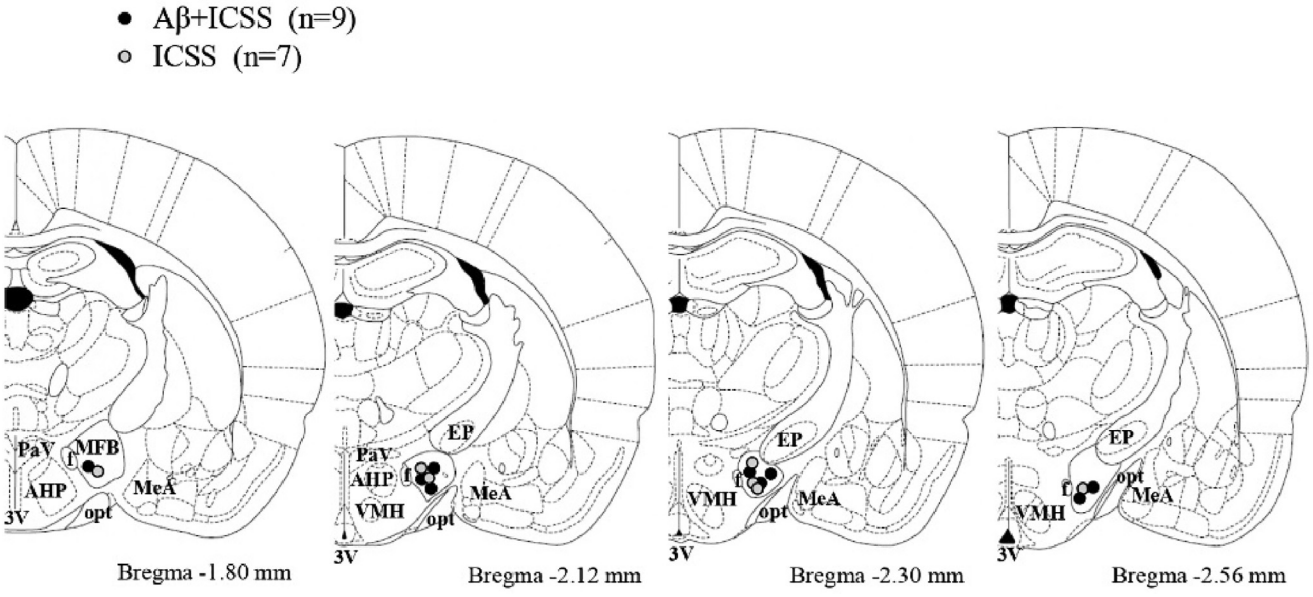

Fig. 5. Location of ICSS electrode at the MFB. Location of the terminal tip of the ICSS stimulation electrodes in the subjects of the Aβ + ICSS and ICSS groups, superimposed on the figures of the Paxinos and Watson atlas at coordinates −1.80 mm to −2.56 mm posterior to Bregma. Abbreviations: AHP: anterior hypothalamic area; EP: entopeduncular nucleus; f: fornix; MeA: medial amygdaloid nucleus; MFB: medial forebrain bundle-lateral hypothalamus; PaV: paraventricular hypothalamic nucleus; opt: optic tract; VMH: ventromedial hypothalamic nucleus; 3 V: 3rd ventricle.

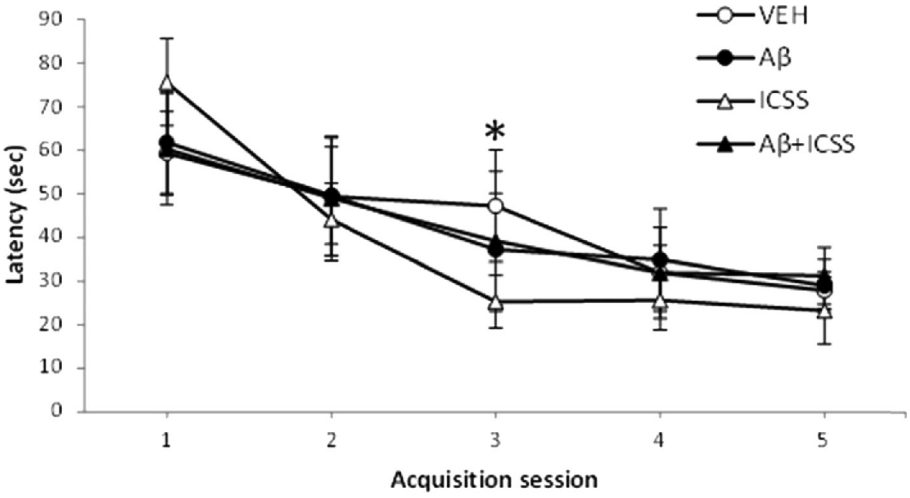

Fig. 6. Effects of Aβ injection and ICSS treatment on spatial task acquisition. Mean escape latencies (±95% confidence interval) for the five acquisition sessions in the MWM. n = 8, 10, 7 and 9 rats/group (VEH, Aβ, ICSS and Aβ + ICSS, respectively). *p < 0.05 ICSS vs VEH.

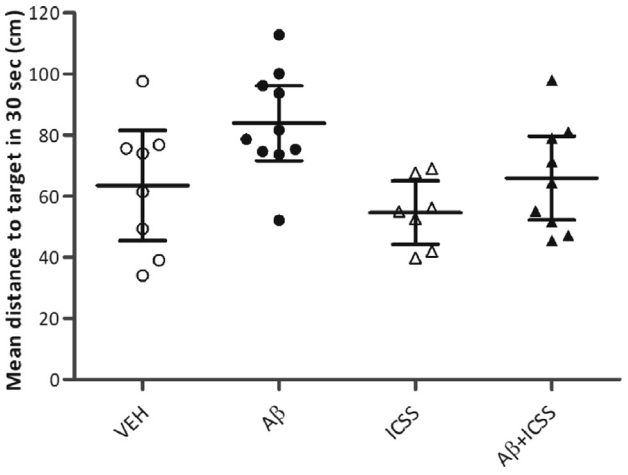

Fig. 7. Effects of ICSS treatment on spatial memory in Aβ-injected rats. Mean distance to target area during the first 30 seconds of the probe test. Each dot represents a single animal. Mean ± 95% confidence interval is depicted. n = 8, 10, 7 and 9 rats/group (VEH, Aβ, ICSS and Aβ + ICSS, respectively). *p < 0.05 vs VEH; #p < 0.05 vs Aβ.

Significant effects for the mean distance to the target area during the first 30 sec of the probe test were observed for both the Aβ ($F_{1,30}$ = 6.833; p < 0.05) and ICSS ($F_{1,30}$ = 4.885; p < 0.05) factors, but not for their interaction. Thus, a general disruptive effect of Aβ,as well as a facilitation by ICSS treatment were observed on the retention at 72 h.. Specifically, rats in the Aβ group showed worse retention than the vehicle ones (p = 0.040; g = 1.009) (Fig. 7). ICSS treatment in Aβ rats not only reduced the mean distance to the target with respect to the Aβ group (p = 0.039; g = 0.981), but also caused similar results to those observed in the VEH group. On the other hand, the percentage of time spent in the target quadrant was similar for all groups. All of them performed above chance level (25%) during both the first 30 seconds [VEH: t_7 = 4.77, p < 0.05; Aβ: t_9 = 3.27, p < 0.05; ICSS: t_6 = 3.38, p < 0.05; Aβ + ICSS: t_8 = 4.57, p < 0.05] and the totality of the trial [VEH: t_7 = 3,51, p < 0.05; Aβ: t_9 = 2.60, p < 0.05; ICSS: t_6 = 3.91, p < 0.05; Aβ + ICSS: t_{11} = 3.78, p < 0.05].

Additionally, no differences were observed between groups in any variable of the cued sessions, indicating that the Aβ animals showed no signs of motor, emotional, or motivational disturbance prior to training that could interfere with escape learning in the MWM. Similarly, effects of Aβ or ICSS treatments on other control variables evaluated in the MWM training sessions, such as time on walls or speed of swimming, were not observed. Finally, no differences were recorded between groups in relation to the type of swimming trajectory in any of the sessions evaluated.

Ptau levels

Aβ-injected rats presented increased ptau levels in layer II of entorhinal cortex [t_{16} = 2.209, p < 0.05; g = 0.998] with respect to VEH, but not in other rhinal cortices, hippocampus or prelimbic cortex. In retrosplenial cortex, a trend towards a significant increase [t_{15} = 2.099, p < 0.05; g = 0.968] was also found in layer III of agranular part in Aβ-injected versus VEH rats. Two-way ANOVA suggests that ICSS treatment had effects on ptau expression in CA1 and CA3 [$F_{1,29}$ = 4.077, p < 0.05 and $F_{1,30}$ = 3.737, p = 0.053, respectively]. In the most distal part of CA1 a significant reduction of ptau levels was found in Aβ + ICSS group with respect to Aβ group (p = 0.046; g = 0.947) (Figs. 8 and 10). In contrast, no effect on ptau levels was found for the ICSS group in this area, despite a reduction of ptau being observed in CA3 (p = 0.042; g = 1.095). Instead, Aβ + ICSS group presented no significant differences relative to VEH group in any region.

No significant correlations were found between ptau levels in any of the analysed regions and impaired behavioural parameters.

DBN levels

Aβ group presented significantly decreased DBN levels with respect to VEH group in layers Ib and II [$t_{,15}$ = 2.246, p < 0.05; g = 1.051 and $t_{,15}$ = 2.584, p < 0.05; g = 1.209, respectively), and a trend [$t_{,15}$ = 2.017, p = 0.062; g = 0.943) to significance pointed at a reduction in layer III of the lateral entorhinal cortex, but not in perirhinal nor ectorhinal cortices (Figs. 9 and 10). DBN levels in these regions showed a significant correlation with the mean distance to the target during the first 30 s of the probe test, in Aβ rats,

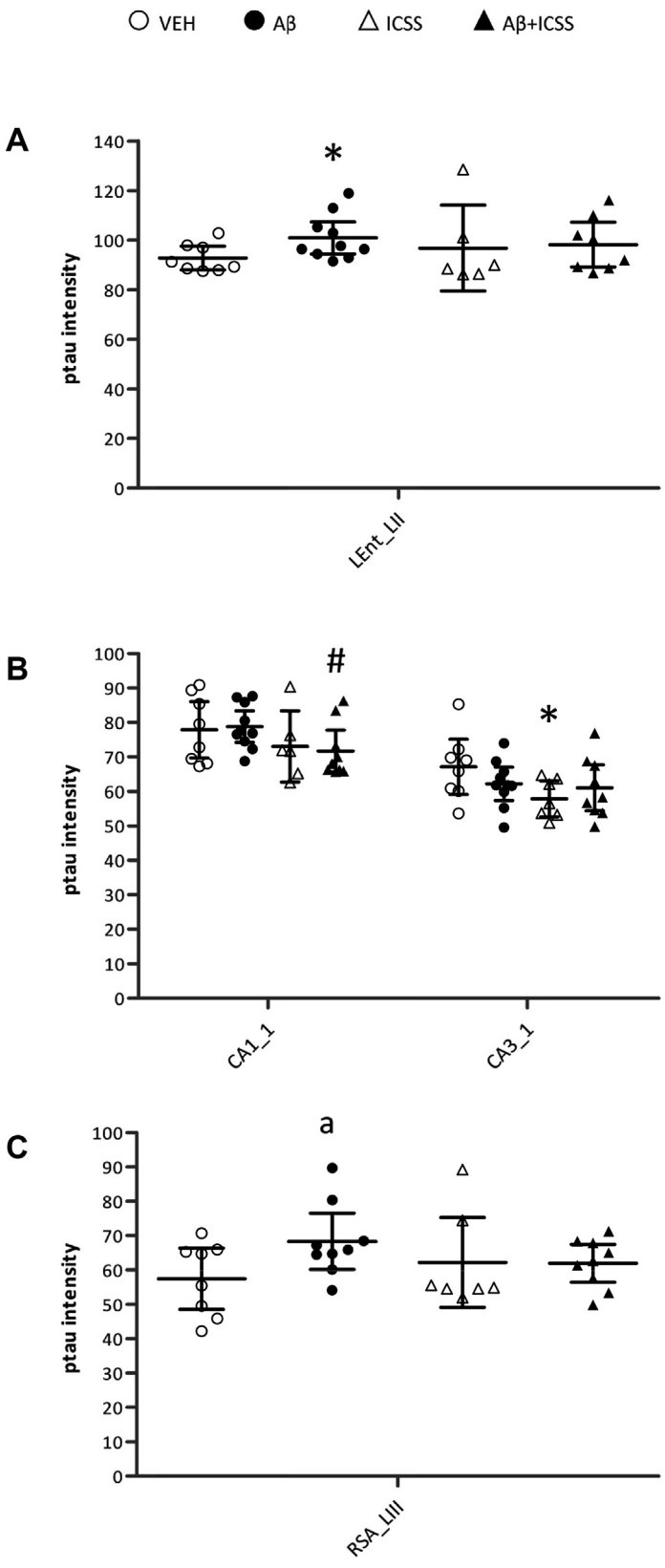

where the rats with higher DBN levels were also the ones with a better performance (Table 1 and Fig. 11). In the hippocampus, a significant reduction was found in the outer molecular layer of suprapyramidal branch in DG [$t_{,15}$ = 3.011, $p < 0.05$; g = 1.408] of Aβ rats, and a trend towards significance [t_{16} = 2.060, $p < 0.05$; g = 0.931] was detected in CA1 *stratum oriens*. A significant decrease was also found in layer I of granular retrosplenial cortex [t_{14} = 2.226, $p < 0.05$; g = 1.060] and in layer III of prelimbic cortex [t_{16} = 2.692, $p < 0.05$; g = 1.216] (Figs. 9 and 10).

In contrast, those rats in the Aβ + ICSS group did not display any significant difference in DBN levels with respect to VEH in any of the studied regions, including those affected in the non-stimulated Aβ group. A statistically significant interaction between the effects of ICSS and Aβ infusion was detected in CA1 *stratum oriens* and trends towards significance were found in DG hilus region [$F_{1,30}$ = 5.754, $p < 0.05$ and $F_{1,30}$ = 3.500, p = 0.070 respectively]. In these two regions, DBN increases were found in Aβ + ICSS rats compared to Aβ rats (p = 0.038; g = 0.880 and p = 0.034; g = 0.901 respectively) (Figs. 9 and 10). Additionally, correlations found in the Aβ group between DBN levels in superficial layers of the entorhinal cortex and behavioural affection disappeared in the Aβ + ICSS group, thus replicating VEH dynamics (Fig. 11).

DISCUSSION

DBS of different brain regions has been suggested as a novel neuromodulatory treatment for AD. Rewarding electrical stimulation aimed at the MFB appears to be a suitable approach to this aim, as MFB-ICSS has been demonstrated to be able to facilitate learning and memory in rodents and to modulate plasticity molecules previously reported to be altered in AD pathology. On this premise, this work assessed for the first time, the effects of post-training MFB-ICSS on spatial learning and memory and on neuropathology molecular markers, including DBN and ptau (at Ser202/Thr205), in a sporadic AD rodent model obtained by Aβ injection.

This study shows that MFB-ICSS treatment consisting of 5 post-training sessions is able to recover the mild spatial memory deficit found in the AD-like rats as well as reverse the aberrant levels of DBN and ptau in specific memory-related areas.

Fig. 8. Effects of Aβ injection and ICSS treatment on ptau levels. Ptau immunohistochemistry staining intensity in the layers and subregions of **(A)** rhinal cortices, **(B)** hippocampus and **(C)** retrosplenial cortex presenting different levels in VEH, Aβ, ICSS and Aβ + ICSS groups after 33 days of Aβ injection. Regions not depicted here did not show different levels of ptau. Each dot represents a single animal. Mean ± 95% confidence interval is depicted. n = 8, 10, 7 and 9 rats/group (VEH, Aβ, ICSS and Aβ + ICSS, respectively). *$p < 0.05$ vs VEH. #$p < 0.05$ vs Aβ; a $p \leq 0.07$ vs VEH. Abbreviations: L: layer; LEnt: lateral entorhinal cortex; RSA: retrosplenial agranular cortex.

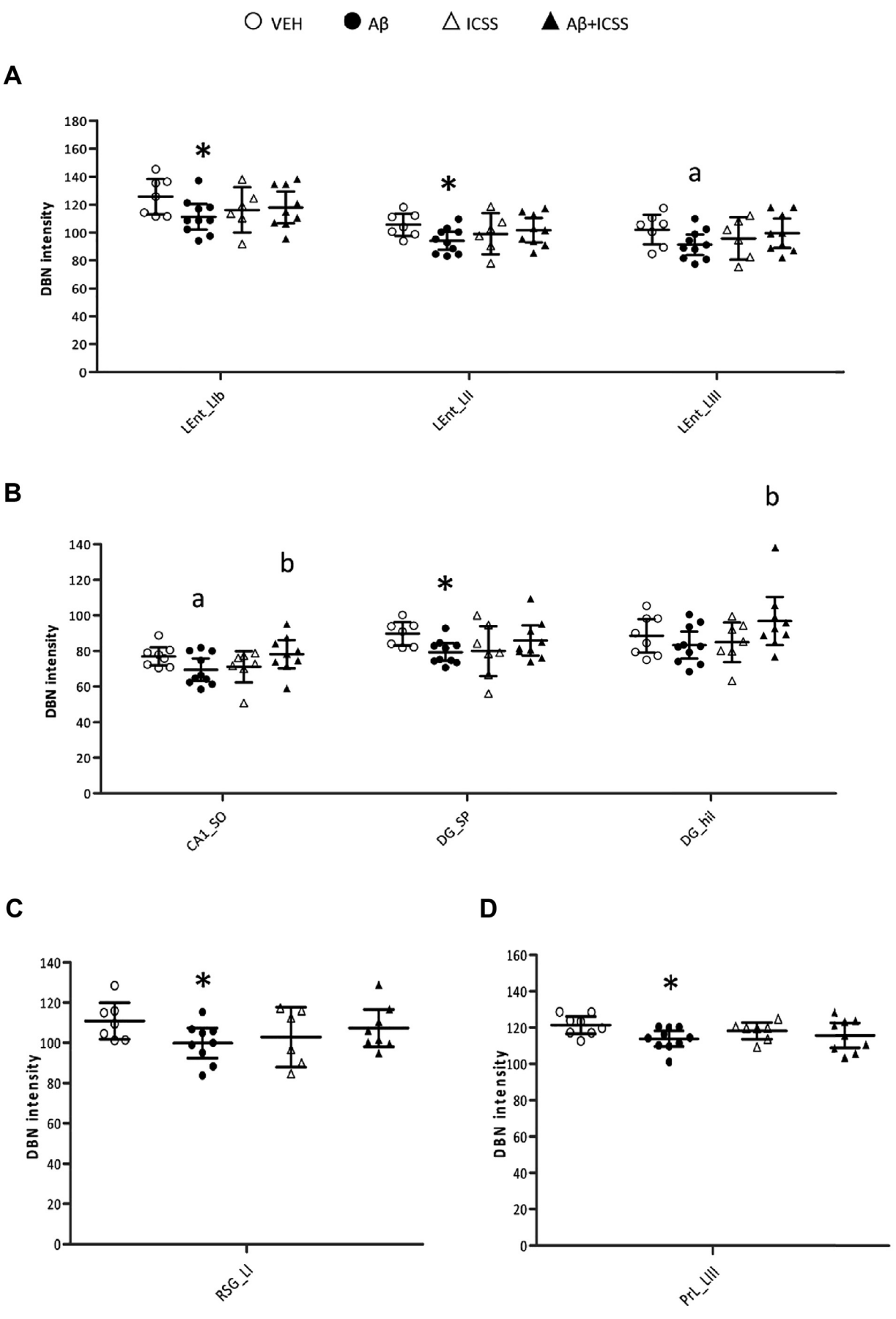
VEH
Aβ
ICSS
Aβ+ICSS
A
DBN intensity
LEnt_LIIb
LEnt_LII
LEnt_LIII
B
CA1_SO
DG_SP
DG_hii
C
RSG_LI
D
PrL_LIII

Injection of amyloid-β into the brain is one of the most extended strategies to model sAD in rodents, sustained by the assumed role of Aβ in triggering AD etiopathology. However, far from being a consistent procedure, a great variety of methodologies leading to different behavioural and neuropathological outcomes have been reported in a great deal of published works. Kasza et al. (2017) addressed the problem of the structural heterogeneity of oligomeric samples testing for different Aβ1-42 aggregation concentration (25, 75 and 200 μM) and at different times (24 and 168 h) and developed an optimized protocol to obtain a sAD rat model by icv injection. They observed spatial memory disturbances, increased ptau immunopositivity, impaired synaptic plasticity (LTP) and decreased neuron viability in the hippocampus, 7 days after Aβ injection, and found the results were more consistent when using 25 μM or 75 μM concentrations and when testing at 168 h in the aggregation process (Kasza et al., 2017). On the basis of these results, the present study used the lower Aβ1-42 aggregation concentration and the longer aggregation time to prepare the toxic oligomers to further characterize its effects on spatial memory and the above-mentioned neuropathological markers at a later time point of 33 days post-injection. Moreover, in addition to the hippocampal region, histopathological hallmarks were assessed in rhinal cortices, including the entorhinal cortex, where AD pathology is generally considered to be initiated, and in the retrosplenial cortex as well as in the prelimbic cortex, where it is thought to progress toward, according to the disconnection hypothesis (Braak and Braak, 1991; Reid and Evans, 2013; Migliaccio et al., 2015).

At a behavioural level, the Aβ group, which was subjected to training at days 26–30 after the injection, did not show significant learning differences regarding control rats in acquisition phase, unlike what was reported at an earlier time point of 7 days (Kasza et al., 2017).

Instead, Aβ rats did show impaired spatial memory retention 72 h later, revealed by differences in mean distance to the target area in the probe test. While this variable has not historically been as popular as latencies when it comes to assessing spatial learning and memory impairment, it is considered a robust variable regarding the assessment of spatial memory accuracy, especially in age-related impairment (Vorhees and Williams, 2006; Gallagher et al., 2015).

Aβ animals also showed changes in the levels of DBN and ptau, which were concentrated in superficial layers of the lateral entorhinal cortex and the hippocampus. Moreover, an exhaustive analysis of the molecular marker levels in the different studied regions and layers showed only slight changes, which is in keeping with descriptions of the initial stage of the disease in humans and transgenic mice (Braak et al., 2006; Khan et al., 2014). Furthermore, DBN levels in the entorhinal cortex correlated with the impaired mean distance to target area of behavioural tests in the Aβ-injected group. This is in line with the idea that synaptic damage correlates more robustly with the degree of cognitive impairment than with the number of amyloid plaques, tangles, and neuronal loss (Ishizuka and Hanamura, 2017). Thus, these results confirm the existence of spatial memory deficit together with the early AD-like regional distribution of taupathology and synaptopathology up to 33 days after an acute low-dose injection of amyloid-β.

In addition, we assessed the effects of a post-training rewarding electrical stimulation treatment targeting the MFB in this early AD model. MFB-ICSS treatment allowed the stimulated animals to reach performance levels similar to those of the control group in fewer training sessions, thus confirming the accelerating effect previously seen in other conditioning paradigms (Aldavert-Vera et al., 1997; Redolar-Ripoll et al., 2003). This effect was not observed in the Aβ rats, which suggests that despite a lack of apparent Aβ-effect on either the acquisition or on the short-term retention of the task, Aβ-injection could partially prevent the facilitating effect of ICSS treatment. Interestingly, a similar outcome was reported after OXR1 blockade (García-Brito et al., 2020).

Remarkably, present results showed that MFB-ICSS treatment reverses 72-h memory impairment observed in this Aβ model. This has also been observed in various paradigms, including in subjects with severe deficits due to brain injuries and after the receptor blockade of some neurochemical systems (Redolar-Ripoll et al., 2003; Segura-Torres et al., 2009; Kádár et al., 2014; García-Brito et al., 2020). Moreover, the persistence of deficits in the explicit spatial memory is in agreement with previous results, also in a sAD model targeting the intralaminar thalamic nucleus (Tsai et al., 2020). In fact, stimulation of both the intralaminar nuclei and the MFB activates multiple brain regions related to cognitive processes such as attention or memory, as revealed by an increased c-fos expression (Shirvalkar et al., 2006; Aldavert-Vera et al., 2013; Kádár et al., 2016). The fornix, the main afference and efference to and from the hippocampal system, has also been used as a target for stimulation treatment to improve memory, in this case in both animals and humans (Ruofan et al., 2022). Although there are no comparative studies in terms of functional efficacy, both bundles -the MFB and the fornix- are related and connect regions that are part of the medial and corticolimbic circuits (Ross et al., 2016; Coenen et al., 2018).

Fig. 9. Effects of Aβ injection and ICSS treatment on DBN levels. DBN immunohistochemistry staining intensity in the layers and subregions of **(A)** rhinal cortices, **(B)** hippocampus, **(C)** retrosplenial cortex and **(D)** prelimbic cortex presenting different levels in VEH, Aβ, ICSS and Aβ + ICSS groups after 33 days of Aβ injection. Regions not depicted here did not show different levels of DBN. Each dot represents a single animal. Mean ± 95% confidence interval is depicted. n = 8, 10, 7 and 9 rats/group (VEH, Aβ, ICSS and Aβ + ICSS, respectively). *$p < 0.05$ vs VEH; a $p \leq 0.07$ vs VEH; b $p \leq 0.07$ vs Aβ. Abbreviations: DG: dentate gyrus; hil: hilus; L: layer; LEnt: lateral entorhinal cortex; PrL: prelimbic cortex; RSG: retrosplenial granular cortex; SP: suprapyramidale.

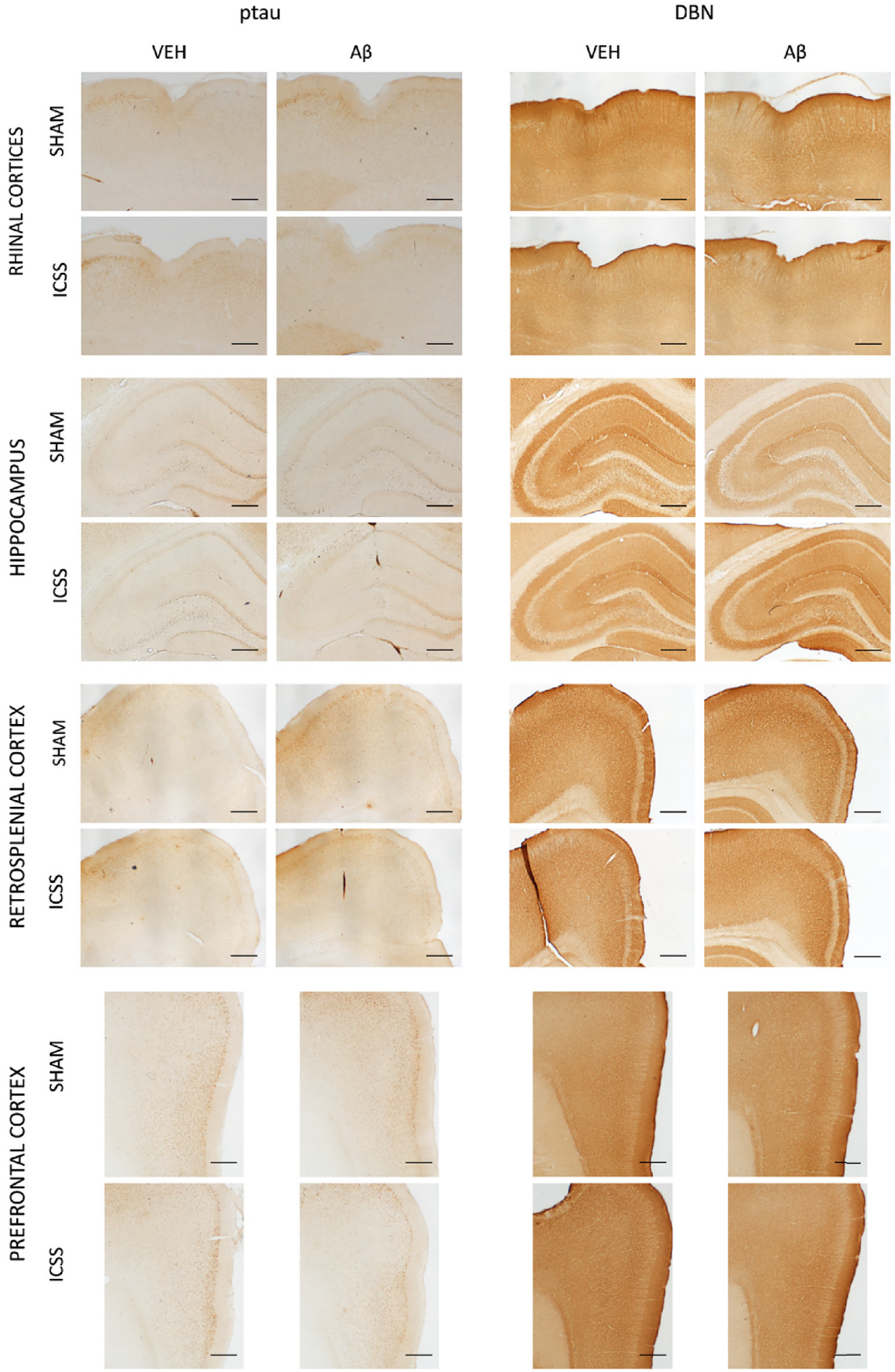

Fig. 10. Effects of Aβ injection and ICSS treatment on ptau and DBN levels. Representative photomicrographs of ptau (left) and DBN (right) immunolabelling in rhinal cortices, hippocampus, retrosplenial cortex and prelimbic cortex, for VEH, Aβ, ICSS and Aβ + ICSS rats, sacrificed 33 days after Aβ injection (scale bar = 500 μm).

Table 1. Correlation analyses between DBN levels in superficial layers of lateral entorhinal cortex and altered behavioural variables 33 days after Aβ injection. Table includes the correlations found significant for the Aβ group, according to Spearman's correlation test ($p < 0.05$, in bold in the table). Correlation with LEnt_LII and mean distance to target is depicted in Fig. 9.

		Mean distance to target in 30 sec	
		Aβ	VEH
DBN intensity levels	LEnt_LIb	*ρ=-.733* **p=.016**	*ρ=-.536* p=.215
	LEnt_LII	*ρ=-.770* **p=.009**	*ρ=-.500* p=.253
	LEnt_LIII	*ρ=-.733* **p=.016**	*ρ=-.179* p=.702

ρ = Spearman's correlation coefficient; n = 7 and 10 rats/group (VEH and Aβ, respectively). Abbreviations: L: layer; LEnt: lateral entorhinal cortex; Mdt: mean distance to target area.

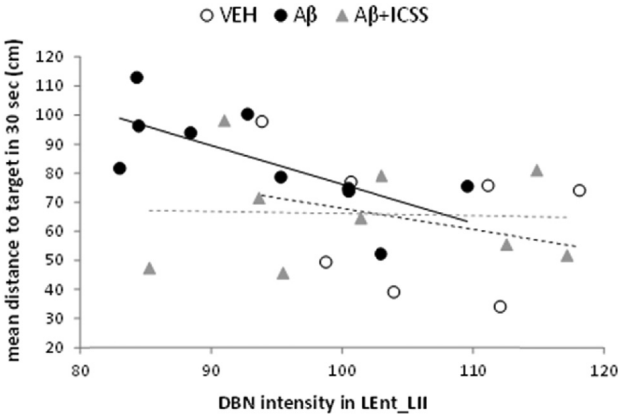

Fig. 11. Scatter plot showing the relation between DBN immunolabelling intensity in layer II of lateral entorhinal cortex with mean distance to target area during the first 30 sec of probe test, in VEH, Aβ and Aβ + ICSS groups, showing loss of correlation in Aβ + ICSS group and approximation to VEH dynamics. Each dot represents a single rat. Spearman's correlation test was used to determine significance ($p < 0.05$). ρ = Spearman's correlation coefficient; n = 7, 10 and 9 rats/group (VEH, Aβ and Aβ + ICSS, respectively). Abbreviations: L: layer; LEnt: lateral entorhinal cortex; Mdt: mean distance to target area.

Interestingly, the activation of the MFB through ICSS manages to compensate for a memory deficit caused by a lesion in the fornix (Yoganarasimha and Meti, 1999). Furthermore, although the fornix can functionally activate reward-related regions such as the nucleus accumbens (Ross et al., 2016), its stimulation has not been shown to cause ICSS behaviour, to our knowledge. In contrast, the MFB is a nuclear component of the brain reward system, and its stimulation results in an easily obtained and persistent ICSS behaviour (Milner, 1991). In fact, MFB has been used as a therapeutic target to treat emotional disorders such as depression and anhedonia (Bewernick et al., 2017; Fenoy et al., 2021) both of which arise in certain phases of Alzheimer's disease (Bennett and Thomas, 2014; Wei et al., 2019). In this context, and without ruling out the importance of the fornix for learning and memory, stimulation of the MFB would have the advantage of being able to affect a wider range of symptoms present in Alzheimer-like neurodegenerative diseases.

Additionally, the present work demonstrates that MFB-ICSS effects in this sAD model are accompanied by a significant decrease of ptau levels in CA1 hippocampal region. This finding is especially interesting considering that the CA1 region has been shown to be the most sensitive hippocampal region in AD (West et al., 1994), after reports of dendritic spine loss and synaptic alterations that characterize the disease (Knobloch and Mansuy, 2008). In this subregion, MFB-ICSS has been previously found to cause long-lasting structural changes, including extended dendritic arborization of pyramidal neurons (Chamorro-López et al., 2015). Furthermore, levels of the postsynaptic protein DBN, involved in dendritic spine morphogenesis, were increased in both CA1 and DG hippocampal subregions of MFB-ICSS-treated Aβ rats, specifically in the same regions where we have previously found that MFB-ICSS upregulates ARC protein (Kádár et al., 2013), a well-known synaptic plasticity marker involved in memory consolidation processes. Thus, these results suggest that MFB-ICSS regulates coordinated molecular mechanisms that overlap with those affected in AD. In this regard, MFB-ICSS modulated the hippocampal expression of specific synaptic plasticity-related microRNAs, such as miR-132, miR-181c and miR-495, and the SIRT1 protein (Puig-Parnau et al., 2020), a deacetylase linked to neuronal health and plasticity during normal aging (Michán et al., 2010; Hadar et al., 2018), all of which have shown alterations in both AD animal models (Schonrock et al., 2010; Hernandez-Rapp et al., 2016) and AD patients (Julien et al., 2009; Wang et al., 2011; Wong et al., 2013; Hadar et al., 2018). In addition, since the DBN, ARC, BDNF, amyloid beta precursor protein (APP) binding family (APPB) as well as the tau tubulin kinase (TTBK) mRNAs have been described as putative targets of the MFB-ICSS-regulated miRNAs (Puig-Parnau et al., 2020), we suggest that these gene expression regulators could be acting as potential mediators of the recovering effects of MFB-ICSS in the AD-like pathological conditions described in this study. To examine this hypothesis, further studies should aim to induce the overexpression and/or downregulation of the miRNAs candidates in the hippocampus of AD rats and analyze the expression of their putative targets and the behavioural effects.

Additionally, although some studies have referred to the synaptic plasticity, neurogenesis and gliogenesis induction as underlying mechanisms of the therapeutic effects of DBS, the timeline of these effects is still an open field of investigation. Some of the clinical trials in AD point out that the deficit is alleviated only temporarily (Lozano et al., 2016) and that the response to stimulation might not be stable over time. This has also been observed in other neuropathological conditions, such as tremor syndromes with long-term aberrant plasticity in cerebellar networks (Peters and Tisch, 2021). Emerging results indicate the potential of alternating stimulation patterns at weekly (Seier et al., 2018) but not at daily inter-

vals (Petry-Schmelzer et al., 2019) in order to improve clinical outcomes after DBS. Therefore, the contribution of further longitudinal follow-up studies in animal models comparing different stimulation programs may be necessary to guide future clinical applications in an attempt to avoid the decline of the beneficial effects of DBS treatments.

In conclusion, the MFB-ICSS treatment was able to reverse both spatial memory deficit as well as neuropathological signs, including ptau increase and DBN decrease in entorhinal cortex and hippocampus, observed in rats 33 days after Aβ injection. To our knowledge, these findings provide the first evidence supporting both cognitive and molecular effects of a rewarding DBS procedure in a sporadic AD model, and they delineate the need to encourage further research into the administration of DBS to the MFB as a potential tool to fight early AD hallmarks from an integrative multifactorial perspective.

CREDIT AUTHORSHIP CONTRIBUTION STATEMENT

Irene Puig-Parnau: Investigation, Formal analysis, Writing – original draft. **Soleil Garcia-Brito:** Investigation, Methodology, Writing – review & editing. **Laia Vila-Soles:** Investigation, Data curation. **Andrea Riberas:** Investigation, Resources. **Laura Aldavert-Vera:** Conceptualization, Methodology, Writing – review & editing. **Pilar Segura-Torres:** Conceptualization, Writing – review & editing, Project administration, Funding acquisition. **Elisabet Kádár:** Conceptualization, Methodology, Writing – review & editing, Supervision, Funding acquisition. **Gemma Huguet:** Conceptualization, Methodology, Supervision, Project administration, Funding acquisition.

ACKNOWLEDGEMENTS

The authors thank Carlos Baldellou Estrada and Cristina Gerboles Freixas for their technical contribution.

FUNDING

This work was supported by PSI2017-83202-C2-1-P and PSI2017-83202-C2-2-P grants from Ministerio de Economía, Indústria y Competitividad (MINECO). I. Puig-Parnau was a recipient of a predoctoral fellowship from the University of Girona (IFUdG2017/61).

ETHICAL APPROVAL

All procedures were performed in accordance with the European Community Council Directive (86/609/CEE, 92/65/CEE, 2010/63/UE) for animal experiments and approved by the Ethics Committee on Animal Welfare of Universitat Autònoma de Barcelona (protocol number 4848 P1) complying with the ARRIVE guidelines.

AUTHOR AGREEMENT

All the authors verify that they concur with the present submission and that the material submitted has not been previously reported in any other journal.

CONFLICT OF INTEREST

The authors declare that they have no conflict of interest.

REFERENCES

Aldavert-Vera L, Costa-Miserachs D, Massané S-Rotger E, Soriano-Mas C, Segura-Torres P, Morgado-Bernal I (1997) Facilitation of a Distributed Shuttle-Box Conditioning with Posttraining Intracranial Self-Stimulation in Old Rats. Neurobiol Learn Mem 67:254–258. https://doi.org/10.1006/nlme.1997.3760.

Aldavert-Vera L, Huguet G, Costa-Miserachs D, Pena S, Ortiz D, Kádár E, Morgado-Bernal I, Segura-Torres P (2013) Intracranial self-stimulation facilitates active-avoidance retention and induces expression of c-Fos and Nurr1 in rat brain memory systems. Behav Brain Res 250:46–57. https://doi.org/10.1016/j.bbr.2013.04.025.

Aldehri M, Temel Y, Alnaami I, Jahanshahi A, Hescham S (2018) Deep brain stimulation for Alzheimer's Disease: An update. Surg Neurol Int 9(58). https://doi.org/10.4103/sni.sni_342_17.

Alzheimer's Association (2019). FDA-approved treatments for Alzheimer's. https://www.alz.org/media/documents/fda-approved-treatments-alzheimers-ts.pdf.

Baldermann JC, Hardenacke K, Hu X, Köster P, Horn A, Freund H-J, Zilles K, Sturm V, Visser-Vandewalle V, Jessen F, Maintz D, Kuhn J (2018) Neuroanatomical Characteristics Associated With Response to Deep Brain Stimulation of the Nucleus Basalis of Meynert for Alzheimer's Disease. Neuromodulat: Technol Neural Interface 21(2):184–190. https://doi.org/10.1111/ner.12626.

Bennett S, Thomas AJ (2014) Depression and dementia: cause, consequence or coincidence? Maturitas 79(2):184–190. https://doi.org/10.1016/J.MATURITAS.2014.05.009.

Bewernick BH, Kayser S, Gippert SM, Switala C, Coenen VA, Schlaepfer TE (2017) Deep brain stimulation to the medial forebrain bundle for depression- long-term outcomes and a novel data analysis strategy. Brain Stimul 10(3):664–671. https://doi.org/10.1016/J.BRS.2017.01.581.

Braak H, Alafuzoff I, Arzberger T, Kretzschmar H, Tredici K (2006) Staging of Alzheimer disease-associated neurofibrillary pathology using paraffin sections and immunocytochemistry. Acta Neuropathol 112(4):389–404. https://doi.org/10.1007/s00401-006-0127-z.

Braak H, Braak E (1991) Neuropathological stageing of Alzheimer-related changes. Acta Neuropathol 82(4):239–259. https://doi.org/10.1007/BF00308809.

Cavanaugh SE, Pippin JJ, Barnard ND (2014) Animal models of Alzheimer disease: Historical pitfalls and a path forward. ALTEX 31(3):279–302. https://doi.org/10.14573/altex.1310071.

Chamorro-López J, Miguéns M, Morgado-Bernal I, Kastanauskaite A, Selvas A, Cabané-Cucurella A, Aldavert-Vera L, DeFelipe J, Segura-Torres P (2015) Structural plasticity in hippocampal cells related to the facilitative effect of intracranial self-stimulation on a spatial memory task. Behav Neurosci 129(6):720–730. https://doi.org/10.1037/bne0000098.

Coenen VA, Schumacher LV, Kaller C, Schlaepfer TE, Reinacher PC, Egger K, Urbach H, Reisert M (2018) The anatomy of the human medial forebrain bundle: Ventral tegmental area connections to reward-associated subcortical and frontal lobe regions. NeuroImage: Clinical 18(March):770–783. https://doi.org/10.1016/j.nicl.2018.03.019.

Fenoy AJ, Quevedo J, Soares JC (2021) Deep brain stimulation of the ''medial forebrain bundle'': a strategy to modulate the reward system and manage treatment-resistant depression. Mol

Psychiatry 2021:1–19. https://doi.org/10.1038/s41380-021-01100-6.
Gallagher M, Burwell RD, Burchinal M (2015) Severity of Spatial Learning Impairment in Aging: Development of a Learning Index for Performance in the Morris Water Maze. Behav Neurosci 129 (4):540–548. https://doi.org/10.1037/bne0000080.
García-Brito S, Morgado-Bernal I, Biosca-Simon N, Segura-Torres P (2017) Intracranial self-stimulation also facilitates learning in a visual discrimination task in the Morris water maze in rats. Behav Brain Res 317:360–366. https://doi.org/10.1016/j.bbr.2016.09.069.
García-Brito S, Aldavert-Vera L, Huguet G, Kádár E, Segura-Torres P (2020) Orexin-1 receptor blockade differentially affects spatial and visual discrimination memory facilitation by intracranial self-stimulation. Neurobiol Learn Mem 169(107188). https://doi.org/10.1016/j.nlm.2020.107188.
Glenner GG, Wong CW (1984) Alzheimer's disease: Initial report of the purification and characterization of a novel cerebrovascular amyloid protein. Biochem Biophys Res Commun 120(3):885–890. https://doi.org/10.1016/S0006-291X(84)80190-4.
Gratwicke J, Zrinzo L, Kahan J, Peters A, Beigi M, Akram H, Hyam J, Oswal A, Day B, Mancini L, Thornton J, Yousry T, Limousin P, Hariz M, Jahanshahi M, Foltynie T (2018) Bilateral deep brain stimulation of the nucleus basalis of meynert for Parkinson disease dementia a randomized clinical trial. JAMA Neurol 75 (2):169–178. https://doi.org/10.1001/jamaneurol.2017.3762.
Grundke-Iqbal I, Iqbal K, Quinlan M, Tung Y-C, Zaidi MS, Wisniewski HM (1986) Microtubule-associated Protein Tau: A component of Alzheimer paired helical filaments. J Biol Chem 261 (13):6084–6089. https://doi.org/10.1016/S0021-9258(17)38495-8.
Grundke-Iqbal I, Iqbal K, Tung Y-C, Quinlan M, Wisniewski HM, Binder LI (1986b) Abnormal phosphorylation of the microtubule-associated protein tau (tau) in Alzheimer cytoskeletal pathology. Proc Natl Acad Sci U S A 83(13):4913–4917. https://doi.org/10.1073/pnas.83.13.4913.
Hadar A, Milanesi E, Walczak M, Puzianowska-Kuźnicka M, Kuźnicki J, Squassina A, Niola P, Chillotti C, Attems J, Gozes I, Gurwitz D (2018) SIRT1, miR-132 and miR-212 link human longevity to Alzheimer's Disease. Sci Rep 8(1):8465. https://doi.org/10.1038/s41598-018-26547-6.
Hardenacke K, Hashemiyoon R, Visser-Vandewalle V, Zapf A, Freund HJ, Sturm V, Hellmich M, Kuhn J (2016) Deep Brain Stimulation of the Nucleus Basalis of Meynert in Alzheimer's Dementia: Potential Predictors of Cognitive Change and Results of a Long-Term Follow-Up in Eight Patients. Brain Stimul 9 (5):799–800. https://doi.org/10.1016/j.brs.2016.05.013.
Hernandez-Rapp J, Rainone S, Goupil C, Dorval V, Smith PY, Saint-Pierre M, Vallée M, Planel E, Droit A, Calon F, Cicchetti F, Hébert SS (2016) microRNA-132/212 deficiency enhances Aβ production and senile plaque deposition in Alzheimer's disease triple transgenic mice. Sci Rep 6:30953. https://doi.org/10.1038/SREP30953.
Huguet G, Aldavert-Vera L, Kádár E, Peña De Ortiz S, Morgado-Bernal I, Segura-Torres P (2009) Intracranial self-stimulation to the lateral hypothalamus, a memory improving treatment, results in hippocampal changes in gene expression. Neuroscience 162:359–374. https://doi.org/10.1016/j.neuroscience.2009.04.074.
Huguet G, Kádár E, Serrano N, Tapias-Espinosa C, García-Brito S, Morgado-Bernal I, Aldavert-Vera L, Segura-Torres P (2020) Rewarding deep brain stimulation at the medial forebrain bundle favours avoidance conditioned response in a remote memory test, hinders extinction and increases neurogenesis. Behav Brain Res 378(112308). https://doi.org/10.1016/j.bbr.2019.112308.
Ishizuka, Y., Hanamura, K. (2017). Drebrin in Alzheimer's disease. In S. Y. Shirao T. (Ed.), Drebrin. Advances in Experimental Medicine and Biology (Vol. 1006, pp. 203–223). https://doi.org/10.1007/978-4-431-56550-5.
Julien C, Tremblay C, Emond V, Lebbadi M, Salem N, Bennett DA, Calon F, Calon F (2009) Sirtuin 1 reduction parallels the accumulation of tau in Alzheimer disease. MAL. J Neuropathol Exp Neurol 68(1):48–58. https://doi.org/10.1097/NEN.0b013e3181922348.
Kádár E, Aldavert-Vera L, Huguet G, Costa-Miserachs D, Morgado-Bernal I, Segura-Torres P (2011) Intracranial self-stimulation induces expression of learning and memory-related genes in rat amygdala. Genes Brain Behav 10:69–77. https://doi.org/10.1111/j.1601-183X.2010.00609.x.
Kádár E, Huguet G, Aldavert-Vera L, Morgado-Bernal I, Segura-Torres P (2013) Intracranial self stimulation upregulates the expression of synaptic plasticity related genes and Arc protein expression in rat hippocampus. Genes Brain Behav 12:771–779. https://doi.org/10.1111/gbb.12065.
Kádár E, Ramoneda M, Aldavert-Vera L, Huguet G, Morgado-Bernal I, Segura-Torres P (2014) Rewarding brain stimulation reverses the disruptive effect of amygdala damage on emotional learning. Behav Brain Res 274:43–52. https://doi.org/10.1016/j.bbr.2014.07.050.
Kádár E, Vico-Varela E, Aldavert-Vera L, Huguet G, Morgado-Bernal I, Segura-Torres P (2016) Increase in c-Fos and Arc protein in retrosplenial cortex after memory-improving lateral hypothalamic electrical stimulation treatment. Neurobiol Learn Mem 128:117–124. https://doi.org/10.1016/j.nlm.2015.12.012.
Kádár E, Vico-Varela E, Aldavert-Vera L, Huguet G, Morgado-Bernal I, Segura-Torres P (2018) Arc protein expression after unilateral intracranial self-stimulation of the medial forebrain bundle is upregulated in specific nuclei of memory-related areas. BMC Neurosci 19(48). https://doi.org/10.1186/s12868-018-0449-5.
Kasza Á, Penke B, Frank Z, Bozsó Z, Szegedi V, Hunya Á, Németh K, Kozma G, Fülöp L (2017) Studies for improving a rat model of Alzheimer's disease: ICV administration of well-characterized β-amyloid 1–42 oligomers induce dysfunction in spatial memory. Molecules (Basel Switzerland) 22(11). https://doi.org/10.3390/molecules22112007.
Khan UA, Liu L, Provenzano FA, Berman DE, Profaci CP, Sloan R, Mayeux R, Duff KE, Small SA (2014) Molecular drivers and cortical spread of lateral entorhinal cortex dysfunction in preclinical Alzheimer's disease. Nat Neurosci 17(2):304–311. https://doi.org/10.1038/nn.3606.
Knobloch M, Mansuy IM (2008) Dendritic spine loss and synaptic alterations in Alzheimer's disease. Mol Neurobiol 37(1):73–82. https://doi.org/10.1007/s12035-008-8018-z.
Kuhn J, Hardenacke K, Lenartz D, Gruendler T, Ullsperger M, Bartsch C, Mai JK, Zilles K, Bauer A, Matusch A, Schulz RJ, Noreik M, Bührle CP, Maintz D, Woopen C, Häussermann P, Hellmich M, Klosterkötter J, Wiltfang J, Maarouf M, Freund HJ, Sturm V (2015) Deep brain stimulation of the nucleus basalis of Meynert in Alzheimer's dementia. Mol Psychiatry 20(3):353–360. https://doi.org/10.1038/mp.2014.32.
Lozano AM, Fosdick L, Chakravarty MM, Leoutsakos J-M, Munro C, Oh E, Drake KE, Lyman CH, Rosenberg PB, Anderson WS, Tang-Wai DF, Pendergrass JC, Salloway S, Asaad WF, Ponce FA, Burke A, Sabbagh M, Wolk DA, Baltuch G, Okun MS, Foote KD, Mcandrews MP, Giacobbe P, Targum SD, Lyketsos CG, Smith GS, St B (2016) A Phase II Study of Fornix Deep Brain Stimulation in Mild Alzheimer's Disease. J Alzheimer's Dis 54:777–787. https://doi.org/10.3233/JAD-160017.
Lv Q, Du A, Wei W, Li Y, Liu G, Wang XP (2018) Deep Brain Stimulation: A Potential Treatment for Dementia in Alzheimer's Disease (AD) and Parkinson's Disease Dementia (PDD). Front Neurosci 12(360). https://doi.org/10.3389/fnins.2018.00360.
Michán S, Li Y, Meng-Hsiu Chou M, Parrella E, Ge H, Long JM, Allard JS, Lewis K, Miller M, Xu W, Mervis RF, Chen J, Guerin KI, Smith LE, McBurney MW, Sinclair DA, Baudry M, de Cabo R, Longo VD (2010) SIRT1 is essential for normal cognitive function and synaptic plasticity. J Neurosci 30(29):9695–9707. https://doi.org/10.1523/JNEUROSCI.0027-10.2010.
Migliaccio R, Agosta F, Possin KL, Canu E, Filippi M, Rabinovici GD, Rosen HJ, Miller BL, Gorno-Tempini ML (2015) Mapping the progression of atrophy in early- and late-onset alzheimer's

disease. J Alzheimer's Dis 46(2):351–364. https://doi.org/10.3233/JAD-142292.
Milner PM (1991) Brain-Stimulation Reward: A Review. Can J Psychol 45(1):1–36.
Paxinos G, Watson C (2006) The Rat Brain in Stereotaxic Coordinates (hard cover). Academic Press.
Peters J, Tisch S (2021) Habituation After Deep Brain Stimulation in Tremor Syndromes: Prevalence, Risk Factors and Long-Term Outcomes. Front Neurol 12(696950). https://doi.org/10.3389/fneur.2021.696950.
Petry-Schmelzer JN, Reker P, Pochmann J, Visser-Vandewalle V, Dembek TA, Barbe MT (2019) Daily Alternation of DBS Settings Does Not Prevent Habituation of Tremor Suppression in Essential Tremor Patients. Mov Disord Clin Pract 6(5):417–418. https://doi.org/10.1002/mdc3.12777.
Puig-Parnau I, Garcia-Brito S, Faghihi N, Gubern C, Aldavert-Vera L, Segura-Torres P, Huguet G, Kádár E (2020) Intracranial Self-Stimulation Modulates Levels of SIRT1 Protein and Neural Plasticity-Related microRNAs. Mol Neurobiol 57(6):2551–2562. https://doi.org/10.1007/s12035-020-01901-w.
Redolar-Ripoll D, Aldavert-Vera L, Soriano-Mas C, Segura-Torres P, Morgado-Bernal I (2002) Intracranial self-stimulation facilitates memory consolidation, but not retrieval: its effects are more effective than increased training. Behav Brain Res 129(1–2):65–75. https://doi.org/10.1016/S0166-4328(01)00325-4.
Redolar-Ripoll D, Soriano-Mas C, Guillazo-Blanch G, Aldavert-Vera L, Segura-Torres P, Morgado-Bernal I (2003) Posttraining intracranial self-stimulation ameliorates the detrimental effects of parafascicular thalamic lesions on active avoidance in young and aged rats. Behav Neurosci 117(2):246–256. https://doi.org/10.1037/0735-7044.117.2.246.
Reid AT, Evans AC (2013) Structural networks in Alzheimer's disease. Eur Neuropsychopharmacol 23(1):63–77. https://doi.org/10.1016/j.euroneuro.2012.11.010.
Ross EK, Kim JP, Settell ML, Han SR, Blaha CD, Min HK, Lee KH (2016) Fornix deep brain stimulation circuit effect is dependent on major excitatory transmission via the nucleus accumbens. Neuroimage 128:138–148. https://doi.org/10.1016/j.neuroimage.2015.12.056.
Ruiz-Medina J, Morgado-Bernal I, Redolar-Ripoll D, Aldavert-Vera L, Segura-Torres P (2008a) Intracranial self-stimulation facilitates a spatial learning and memory task in the Morris water maze. Neuroscience 154(2):424–430. https://doi.org/10.1016/j.neuroscience.2008.03.059.
Ruiz-Medina J, Redolar-Ripoll D, Morgado-Bernal I, Aldavert-Vera L, Segura-Torres P (2008b) Intracranial self-stimulation improves memory consolidation in rats with little training. Neurobiol Learn Mem 89:574–581. https://doi.org/10.1016/j.nlm.2007.11.005.
Ruofan L, Chencheng Z, Yanxia R, Ti-Fei Y (2022) Deep Brain stimulation of fornix for memory improvement in Alzheimer's disease: A critical review. Ageing research reviews 79:1–12. https://doi.org/10.1016/j.arr.2022.101668.
Schonrock N, Ke YD, Humphreys D, Staufenbiel M, Ittner LM, Preiss T, Tz RG, J. (2010) Neuronal MicroRNA Deregulation in Response to Alzheimer's Disease Amyloid-b. PLoS One 5(6):e11070.
Segura-Torres P, Capdevila-Ortís L, Martí-Nicolovius M, Morgado-Bernal I (1988) Improvement of shuttle-box learning with pre- and post-trial intracranial self-stimulation in rats. Behav Brain Res 29(1–2):111–117. https://doi.org/10.1016/0166-4328(88)90058-7.
Segura-Torres P, Aldavert-Vera L, Gatell-Segura A, Redolar-Ripoll D, Morgado-Bernal I (2009) Intracranial self-stimulation recovers learning and memory capacity in basolateral amygdala-damaged rats. Neurobiol Learn Mem 93:117–126. https://doi.org/10.1016/j.nlm.2009.09.001.
Seier M, Hiller A, Quinn J, Murchison C, Brodsky M, Anderson S (2018) Alternating Thalamic Deep Brain Stimulation for Essential Tremor: A Trial to Reduce Habituation. Mov Disord Clin Pract 5(6):620–626. https://doi.org/10.1002/mdc3.12685.
Selkoe DJ (2002) Alzheimer's disease is a synaptic failure. Science 298(5594):789–791. https://doi.org/10.1126/science.1074069.
Shirvalkar P, Seth M, Schiff ND, Herrera DG (2006) Cognitive enhancement with central thalamic electrical stimulation. PNAS 103(45):17007–17012. https://doi.org/10.1073/pnas.0604811103.
Soriano-Mas C, Redolar-Ripoll D, Aldavert-Vera L, Morgado-Bernal I, Segura-Torres P (2005) Post-training intracranial self-stimulation facilitates a hippocampus-dependent task. Behav Brain Res 160:141–147. https://doi.org/10.1016/j.bbr.2004.11.025.
Terry RD (2000) Cell death or synaptic loss in Alzheimer disease. J Neuropathol Exp Neurol 59(12):1118–1119. https://doi.org/10.1093/jnen/59.12.1118.
Tsai ST, Chen SY, Lin SZ, Tseng GF (2020) Rostral intralaminar thalamic deep brain stimulation ameliorates memory deficits and dendritic regression in β-amyloid-infused rats. Brain Struct Funct 225(2):751–761. https://doi.org/10.1007/S00429-020-02033-6.
Vorhees CV, Williams MT (2006) Morris water maze: Procedures for assessing spatial and related forms of learning and memory. Nat Protoc 1(2):848–858. https://doi.org/10.1038/nprot.2006.116.
Vorhees CV, Williams MT (2010) Morris water maze: procedures for assessing spatial and related forms of learning and memory. Nat Protoc 1(2):848–858. https://doi.org/10.1038/nprot.2006.116.Morris.
Wang WX, Huang Q, Hu Y, Stromberg AJ, Nelson PT (2011) Patterns of microRNA expression in normal and early Alzheimer's disease human temporal cortex: White matter versus gray matter. Acta Neuropathol 121(2):193–205. https://doi.org/10.1007/s00401-010-0756-0.
Wei G, Irish M, Hodges JR, Piguet O, Kumfor F (2019) Disease-specific profiles of apathy in Alzheimer's disease and behavioural-variant frontotemporal dementia differ across the disease course. J Neurol 267(4):1086–1096. https://doi.org/10.1007/S00415-019-09679-1.
Weintraub S, Wicklund AH, Salmon DP (2012) The neuropsychological profile of Alzheimer disease. Cold Spring Harb Perspect Med 2(4). https://doi.org/10.1101/cshperspect.a006171.
West MJ, Coleman PD, Flood DG, Troncoso JC (1994) Differences in the pattern of hippocampal neuronal loss in normal ageing and Alzheimer's disease. Lancet 344(8925):769–772. https://doi.org/10.1016/S0140-6736(94)92338-8.
Wong HKA, Veremeyko T, Patel N, Lemere CA, Walsh DM, Esau C, Vanderburg C, Krichevsky AM (2013) De-repression of FOXO3a death axis by microRNA-132 and -212 causes neuronal apoptosis in Alzheimer's disease. Hum Mol Genet 22(15):3077–3092. https://doi.org/10.1093/hmg/ddt164.
Yoganarasimha D, Meti BL (1999) Amelioration of fornix lesion induced learning deficits by self-stimulation rewarding experience. Brain Res 845(2):246–251. https://doi.org/10.1016/S0006-8993(99)01957-5.
Yu D, Yan H, Zhou J, Yang X, Lu Y, Han Y (2019) A circuit view of deep brain stimulation in Alzheimer 's disease and the possible mechanisms. Mol Neurodegener 14(33):1–12. https://doi.org/10.1186/s13024-019-0334-4.
Zhang L, Chen C, Mak MS, Lu J, Wu Z, Chen Q, Han Y, Li Y, Pi R (2019) Advance of sporadic Alzheimer's disease animal models. Med Res Rev 40:431–458. https://doi.org/10.1002/med.21624.

(Received 9 May 2022, Accepted 5 January 2023)
(Available online 14 January 2023)